# Supporting Information

**Hybrid chemical vapor deposition enables scalable and stable Cs-FA mixed cation perovskite solar modules with a designated area of 91.8 cm$^2$ approaching 10% efficiency**

*Longbin Qiu,†[a] Sisi He,†[a] Yan Jiang,[a] Dae-Yong Son,[a] Luis K. Ono,[a] Zonghao Liu,[a] Taehoon Kim,[a] Theodoros Bouloumis,[a] Said Kazaoui,[b] Yabing Qi*[a]*

† L. Qiu and S. He contributed equally to this work.

a. Energy Materials and Surface Sciences Unit (EMSSU), Okinawa Institute of Science and Technology Graduate University (OIST), 1919-1 Tancha, Kunigami-gun, Onna-son, Okinawa 904-0495, Japan.
*Corresponding author: Yabing Qi, E-mail: Yabing.Qi@OIST.jp

b. Research Center for Photovoltaics (RCPV), National Institute of Advanced Industrial Science and Technology (AIST), Tsukuba, Ibaraki 305-8565, Japan

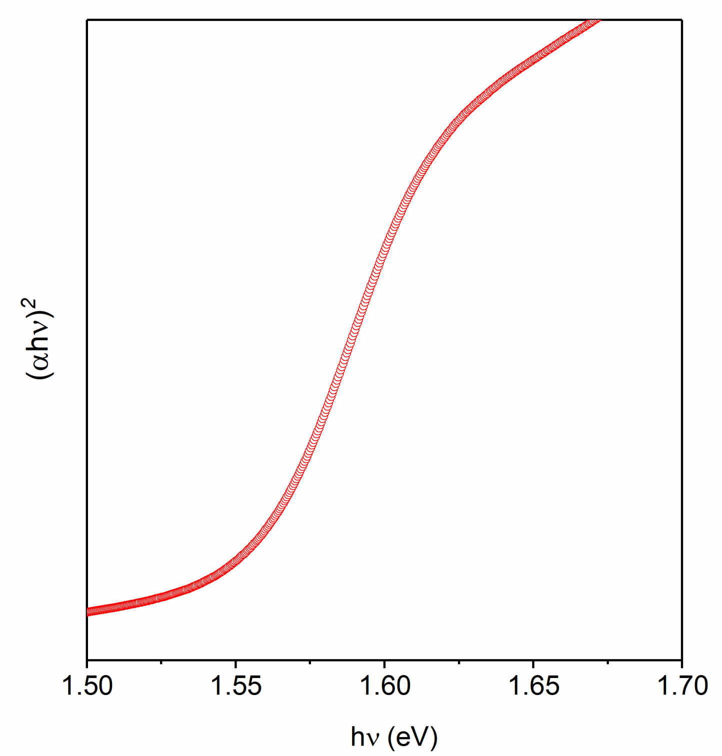


**Figure S1. Tauc-plot of the $Cs_{0.1}FA_{0.9}PbI_{2.9}Br_{0.1}$ perovskite film exhibiting an optical band-gap of 1.56 eV.**

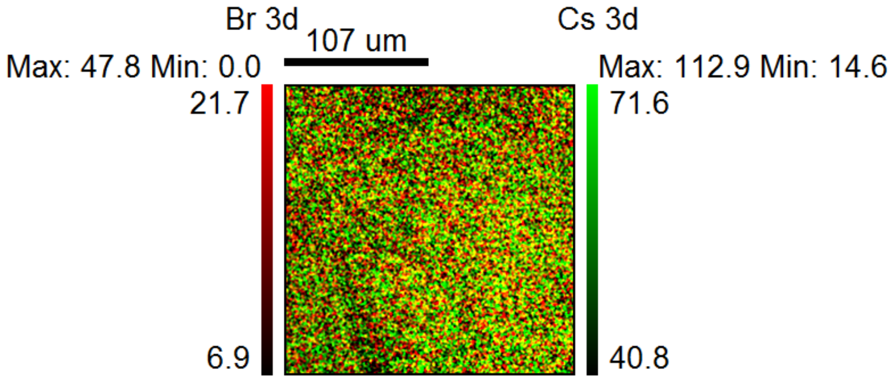


**Figure S2. XPS mapping of the $Cs_{0.1}FA_{0.9}PbI_{2.9}Br_{0.1}$ perovskite layer, which shows the uniform distribution of Br and Cs elements.**

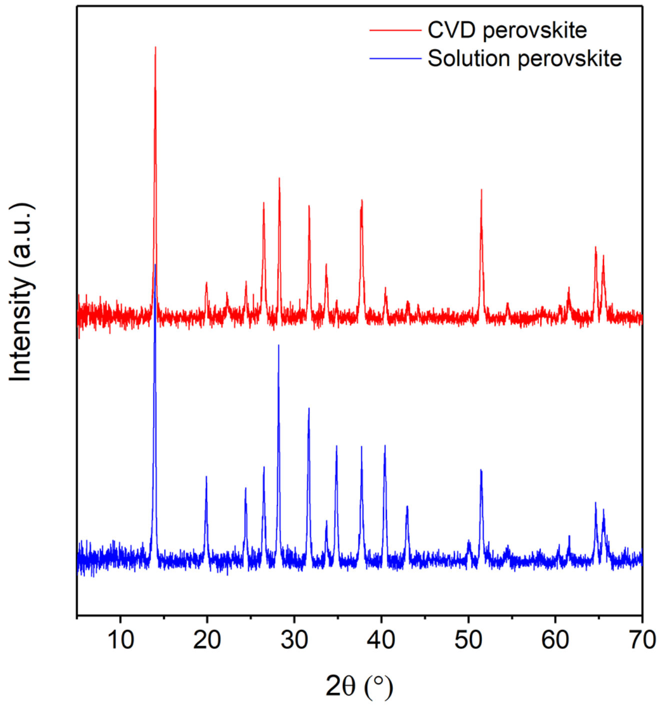


**Figure S3. XRD data of the $Cs_{0.1}FA_{0.9}PbI_{2.9}Br_{0.1}$ perovskite film by the CVD process and the solution coating process.**

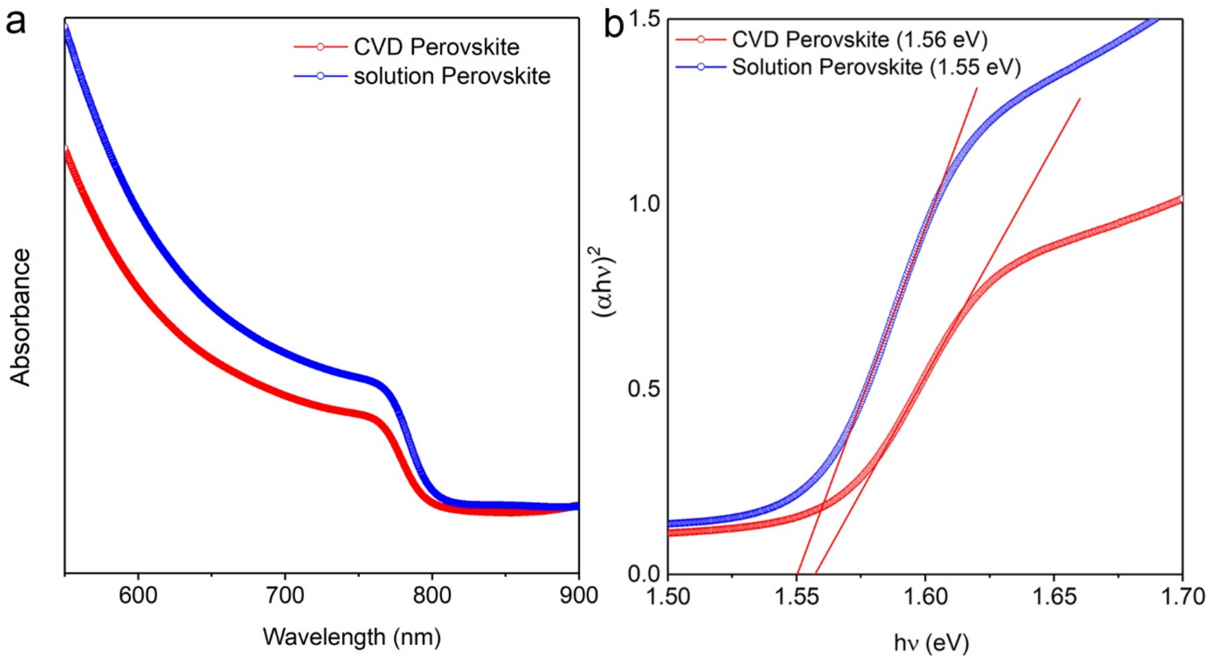


**Figure S4. a)** Absorbance and the corresponding **b)** Tauc-plots of the $Cs_{0.1}FA_{0.9}PbI_{2.9}Br_{0.1}$ perovskite films by the CVD process and the solution coating process.

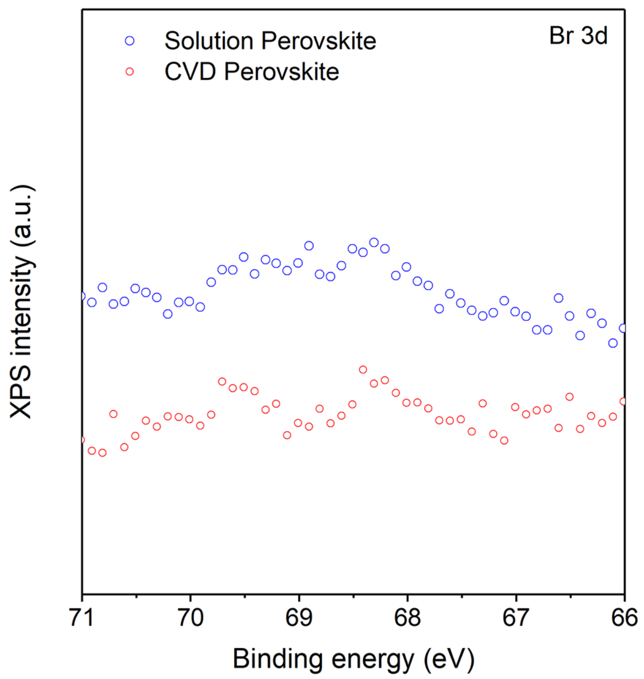


**Figure S5. XPS spectra of the Br 3d core level of the $Cs_{0.1}FA_{0.9}PbI_{2.9}Br_{0.1}$ perovskite film by the CVD process and the solution coating process.**

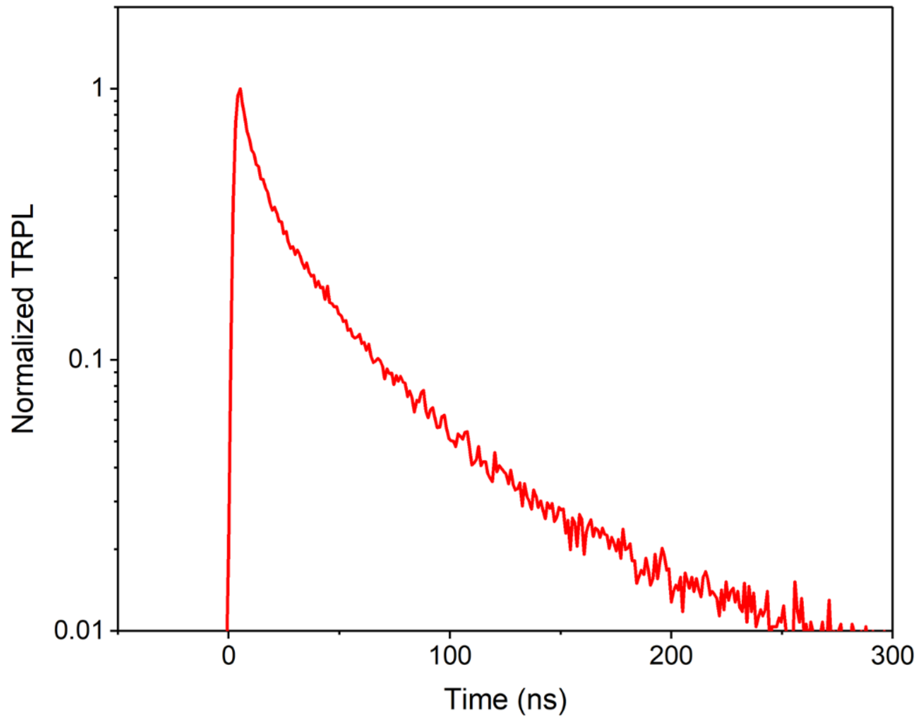


**Figure S6. Time-resolved photoluminescence data of the $Cs_{0.1}FA_{0.9}PbI_{2.9}Br_{0.1}$ perovskite film on glass and measured in air.** The limitation of open-circuit voltage due to recombination is 1.04 V.[S1]

**Supporting Note 1.**

To calculate the $V_{OC}$ limitation due to the non-radiative recombination, we refer to the process described by W. Tress and the example applied by D. Neher et al.[S1]

$$eV_{oc} = E_g + k_B T * \ln\left(\frac{n_e n_h}{N_c N_v}\right) \quad (1)$$

$$\frac{dn_e}{d_t} = G - R \rightarrow 0 \sim G - \frac{n_e}{\tau} \rightarrow n_e \sim G\tau \quad (2)$$

$$G \sim \frac{J_{sc}}{ed} \quad (3)$$

$$N_C = 2[\frac{2\pi m_e^* k_B T}{h^2}]^{3/2} \quad (4)$$

$$N_V = 2[\frac{2\pi m_h^* k_B T}{h^2}]^{3/2} \quad (5)$$

Here, $E_g$ is the band gap of perovskite (1.56 eV); $k_B$ is the Boltzmann constant; T is the temperature ($K$); $n_e$ ($n_h$) is the density of electrons (holes) in the conduction (valance) band; $N_C$ ($N_V$) is the effective density of states in the conduction (valence) band ($3.12 \times 10^{24}$ /m$^3$); $m_e^*$ ($m_h^*$) is the effective mass for electrons (holes). $G$ is the generation rate and $R$ is the recombination rate. Assuming equal densities for electrons and holes and using τ = 30 ns extracted from **Figure S6**, the achievable $V_{OC}$ is 1.04 V.

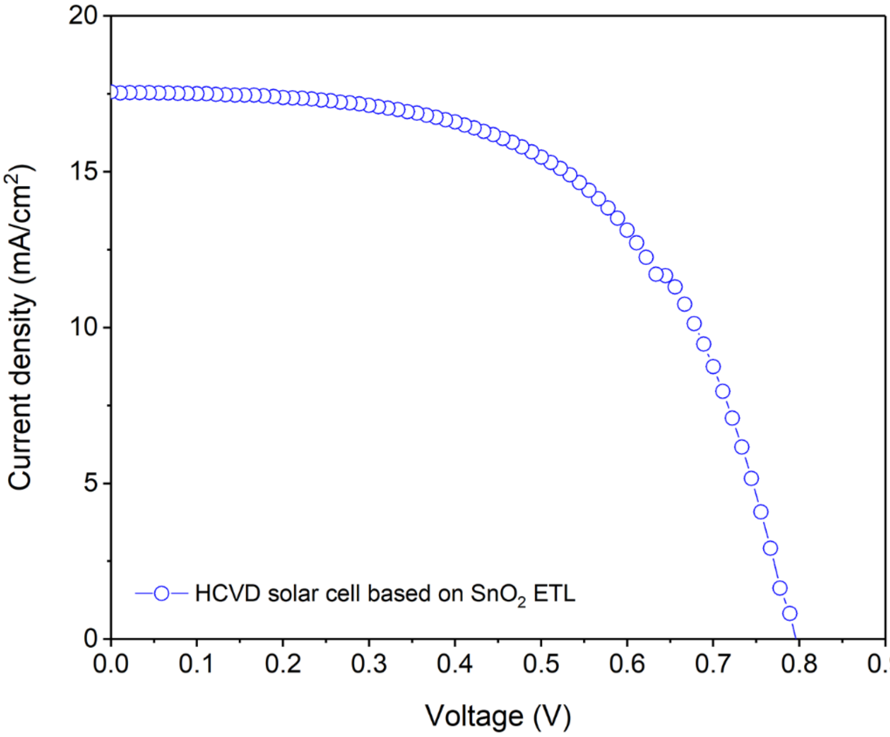


**Figure S7. Typical J-V curves with sputtered $SnO_2$ as electron transport layer for the HCVD grown perovskite $Cs_{0.1}FA_{0.9}PbI_{2.9}Br_{0.1}$ based devices.**

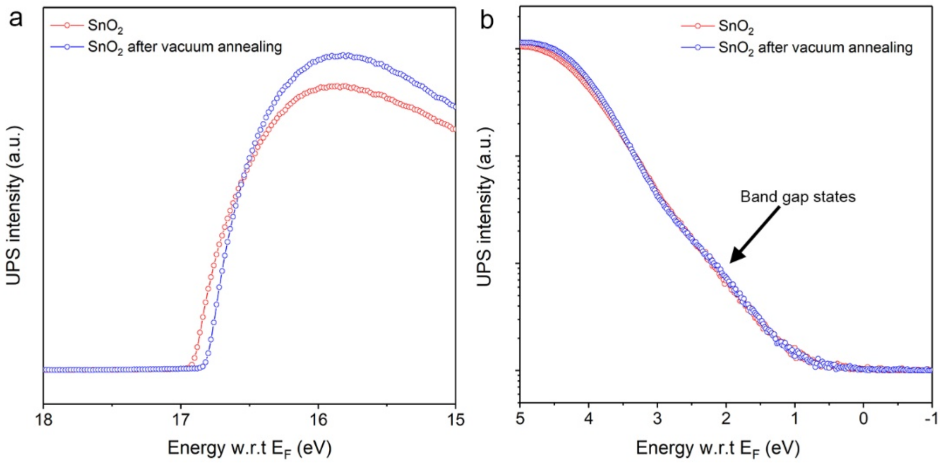


**Figure S8. Secondary electron cutoff (work function determination) and valance band spectra (shown in log scale) of the $SnO_2$ film before and after the vacuum annealing process.**

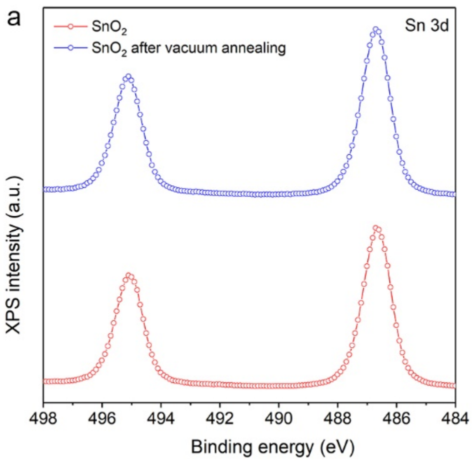


**Figure S9. XPS a) Sn 3d and b) O 1s core level spectra of the $SnO_2$ film before and after vacuum annealing.** After vacuum annealing the O content decreased by 4% (with the Sn content normalized to 1).

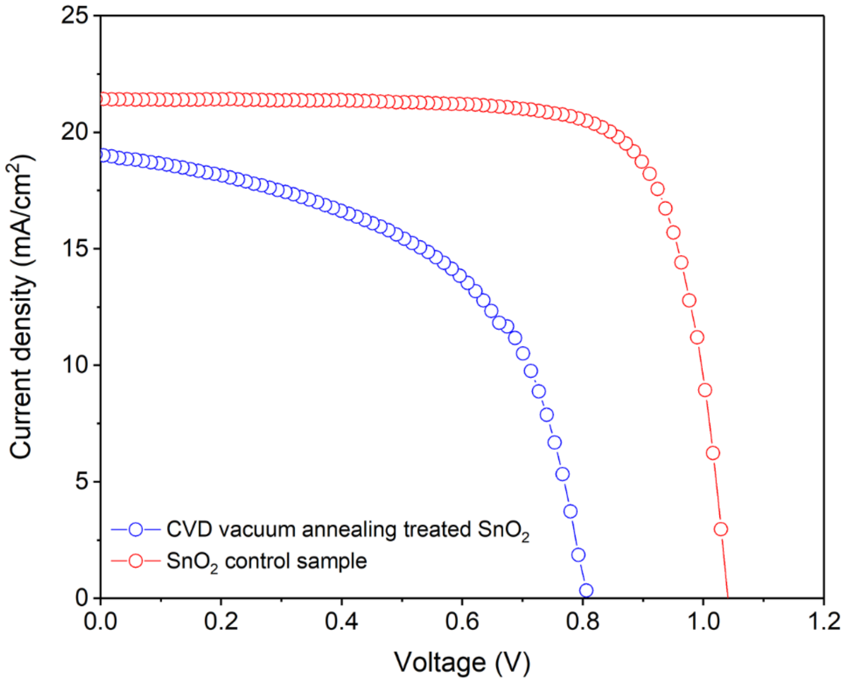


**Figure S10. Typical J-V curves with $SnO_2$ and vacuum annealed $SnO_2$ as electron transport layer for spin coated perovskite based devices.**

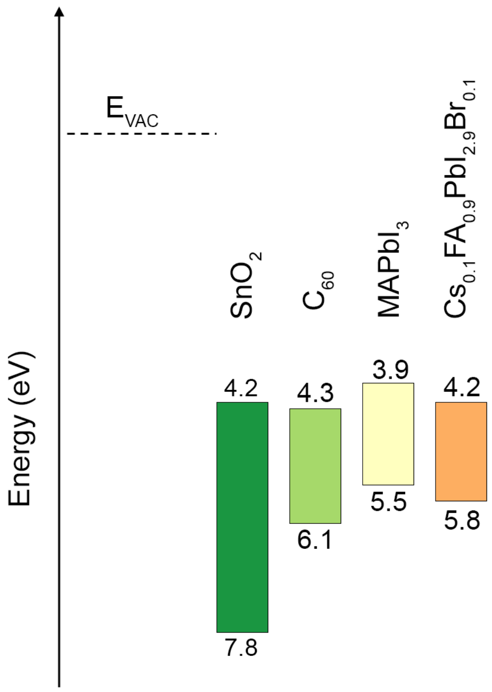


**Figure S11. Energy level diagram of perovskite solar cells with the vacuum deposited $SnO_2/C_{60}$ electron transport layer and the HCVD grown $MAPbI_3$ and $Cs_{0.1}FA_{0.9}PbI_{2.9}Br_{0.1}$ perovskite materials.**

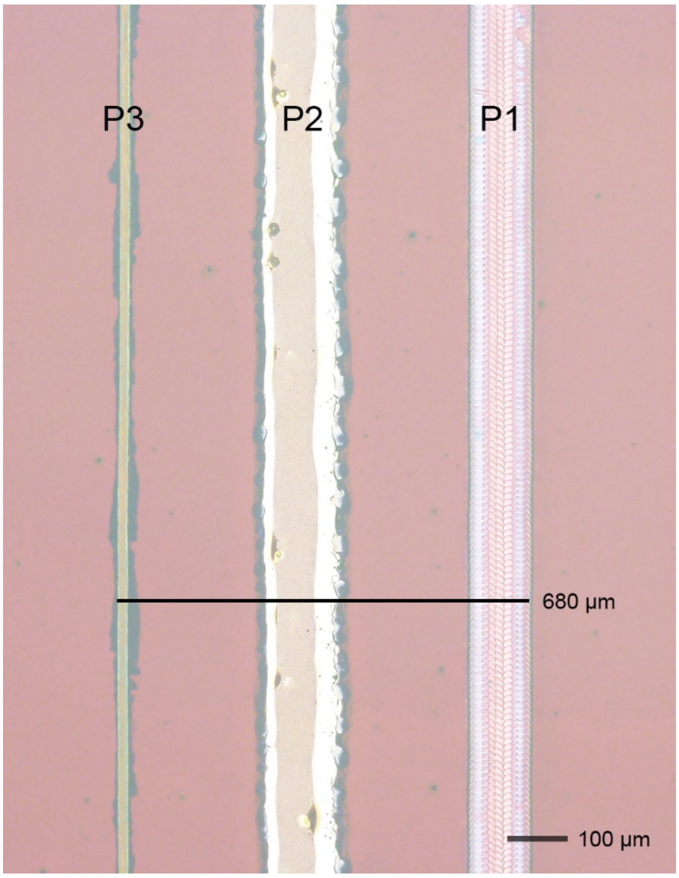

**Figure S12. Solar module patterning for sub-cell interconnection with a geometric fill factor of 0.9.**

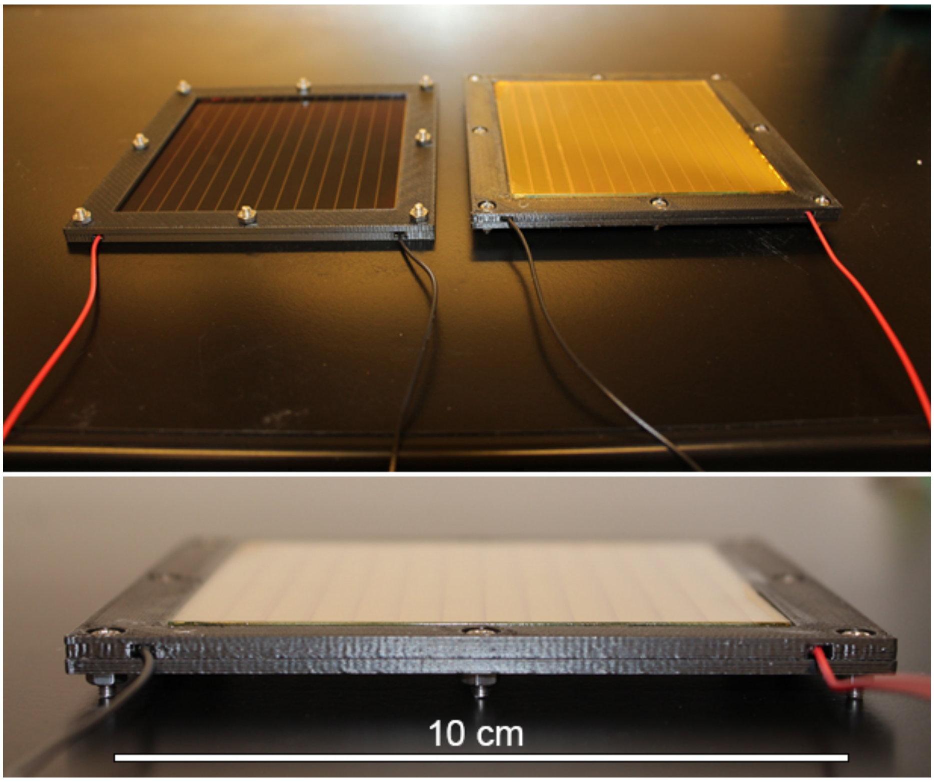


**Figure S13. Side view of the perovskite solar modules after encapsulation.**

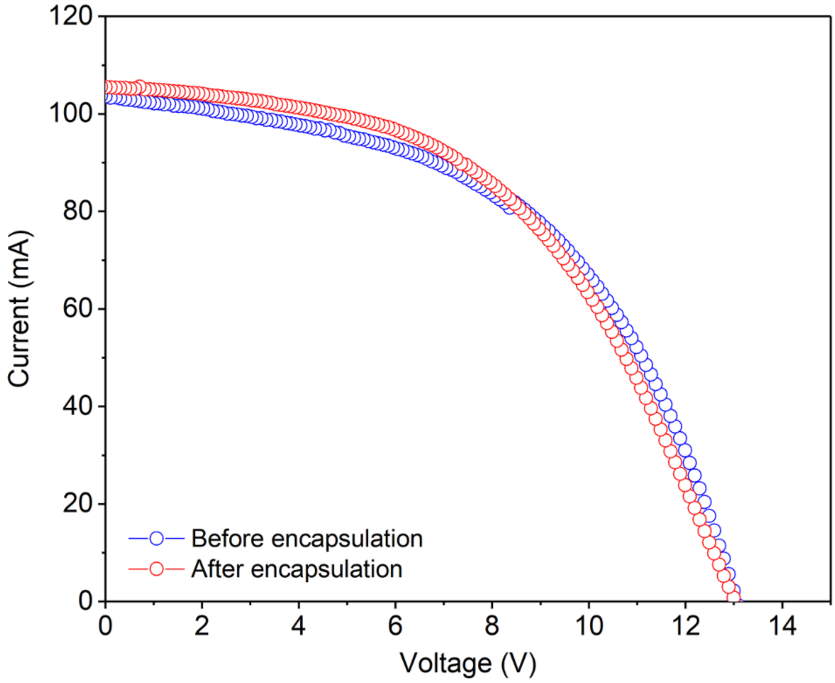


**Figure S14. 10 cm × 10 cm $Cs_{0.1}FA_{0.9}PbI_{2.9}Br_{0.1}$ solar module performance before and after encapsulation.**

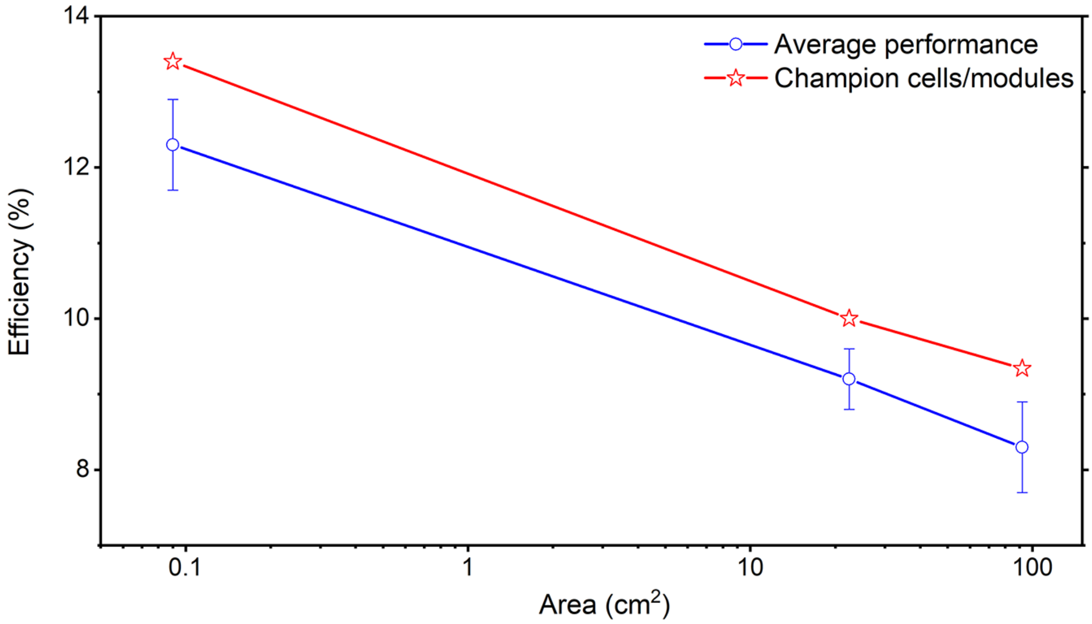


**Figure S15. Solar cell efficiency decays as a function of cell/module designated area for both champion and average solar cell/module performance (decay rate 1.3% per decade).**

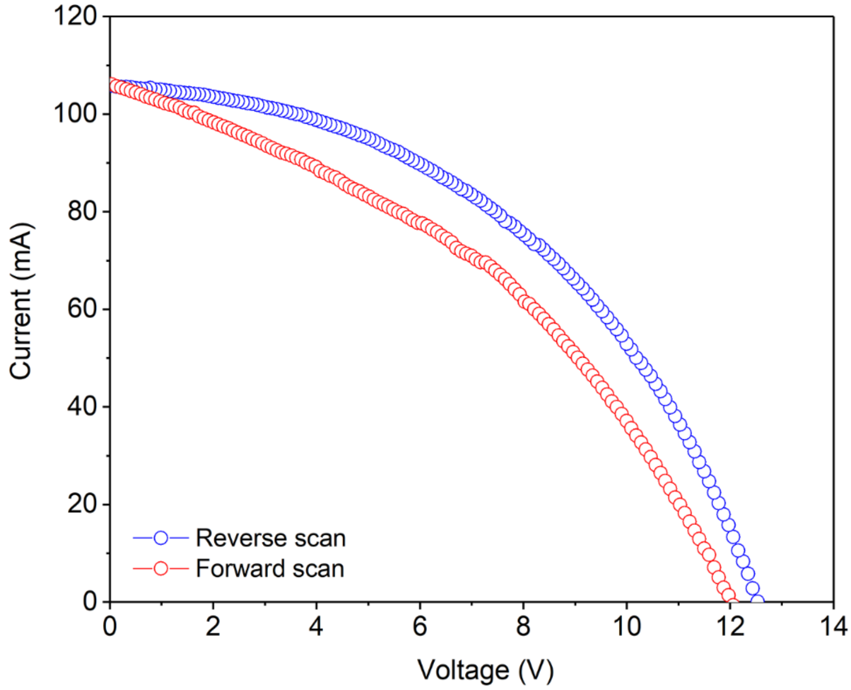


**Figure S16. Hysteresis of the HCVD fabricated $Cs_{0.1}FA_{0.9}PbI_{2.9}Br_{0.1}$ solar module with an area of 10 cm × 10 cm.**

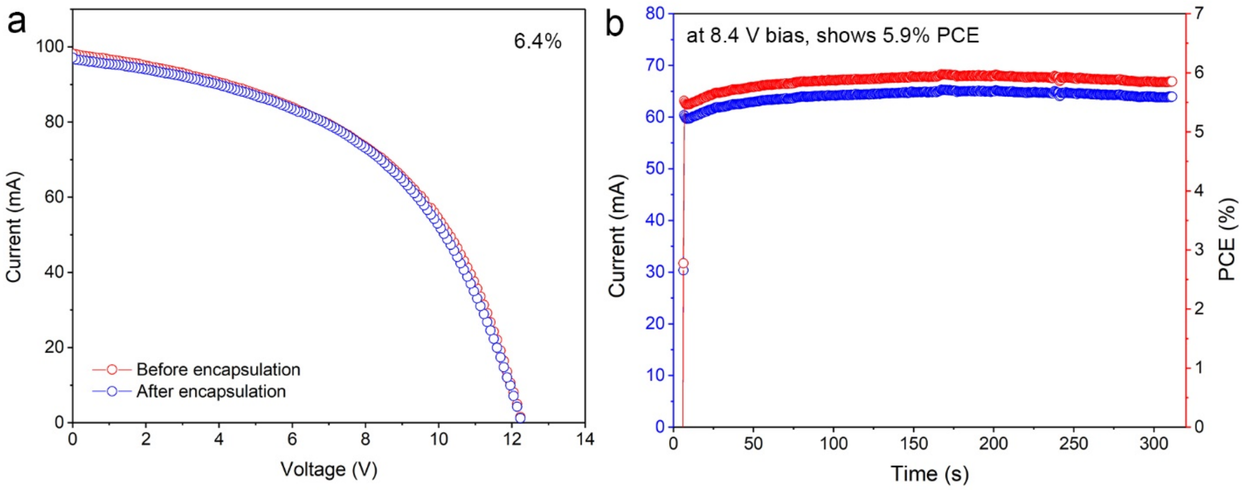


**Figure S17. 10 cm × 10 cm HCVD fabricated $MAPbI_3$ solar module performance. a.** J-V curves before and after encapsulation shows a similar PCE of approximately 6.4%. **b.** Steady-state power output at the bias voltage of 8.4 V shows the stabilized PCE of 5.9%.

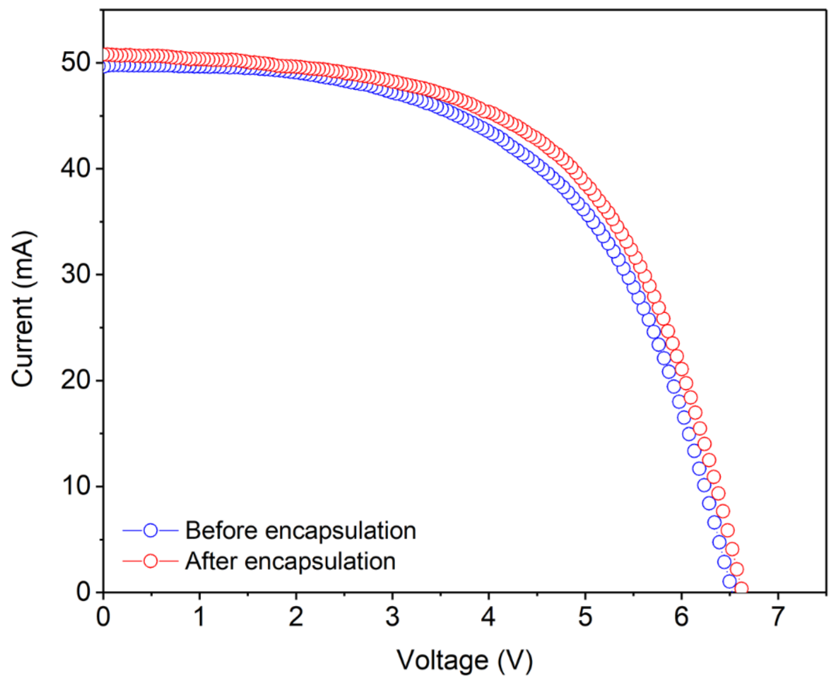


**Figure S18. 5 cm × 5 cm solar module performance before and after encapsulation.**

**Table S1. Binding energy for the XPS core levels of Cs 3d and Pb 4f before and after HCVD.**

| | Cs 3d3/2 (eV) | Cs 3d5/2 (eV) | Pb 4f5/2 (eV) | Pb 4f7/2 (eV) |
|---|---|---|---|---|
| $PbI_2$/CsBr | 738.1 | 724.2 | 142.8 | 137.9 |
| $Cs_{0.1}FA_{0.9}PbI_{2.9}Br_{0.1}$ | 738.8 | 724.8 | 143.2 | 138.3 |

**Table S2. Photovoltaic parameters for the HCVD fabricated devices based on $SnO_2$ and $SnO_2/C_{60}$ electron transport layer.**

| ETL | $V_{OC}$ (V) | $J_{SC}$ (mA/cm$^2$) | FF | PCE (%) |
|---|---|---|---|---|
| $SnO_2$ | 0.81 ± 0.07 | 18.4 ± 0.5 | 0.54 ± 0.04 | 8.1 ± 1.1 |
| $SnO_2/C_{60}$ | 0.90 ± 0.04 | 20.2 ± 0.3 | 0.67 ± 0.02 | 12.3 ± 0.6 |

**Table S3. Photovoltaic parameters for the solution coated perovskite devices based on different $SnO_2$ with and without the vacuum annealing treatment.**

| | $SnO_2$ treatment | $V_{OC}$ (V) | $J_{SC}$ ($mA/cm^2$) | FF | PCE (%) |
|---|---|---|---|---|---|
| Sputtered $SnO_2$ | Without vacuum annealing | 1.03 ± 0.01 | 21.4 ± 0.2 | 0.74 ± 0.02 | 16.4 ± 0.5 |
| | With vacuum annealing | 0.73 ± 0.04 | 18.8 ± 0.9 | 0.55 ± 0.02 | 7.6 ± 0.6 |
| Alfa Aesar $SnO_2$ (solution coating) | Without vacuum annealing | 1.06 ± 0.01 | 20.2 ± 0.3 | 0.72 ± 0.04 | 15.5 ± 0.8 |
| | With vacuum annealing | 0.96 ± 0.02 | 19.6 ± 0.2 | 0.62 ± 0.04 | 11.7 ± 0.9 |
| $SnO_2/C_{60}$ | Without vacuum annealing | 1.02 ± 0.01 | 20.7 ± 0.6 | 0.68 ± 0.02 | 14.4 ± 0.7 |
| | With vacuum annealing | 1.00 ± 0.02 | 20.6 ± 0.5 | 0.66 ± 0.03 | 13.6 ± 0.7 |

**Table S4. Photovoltaic parameters for the 10 cm × 10 cm perovskite solar modules with a designated area of 91.8 $cm^2$ fabricated using the HCVD method.**

| Number | $V_{OC}$ (V) | $J_{SC}$ ($mA/cm^2$) | FF | PCE (%) |
|---|---|---|---|---|
| 1 | 12.92 | 1.17 | 0.53 | 8.06 |
| 2 | 12.60 | 1.10 | 0.56 | 7.74 |
| 3 | 13.04 | 1.22 | 0.58 | 9.17 |
| 4 | 12.54 | 1.22 | 0.55 | 8.40 |
| 5 | 12.34 | 1.21 | 0.52 | 7.83 |
| 6 | 12.44 | 1.19 | 0.56 | 8.37 |
| 7 | 12.49 | 1.19 | 0.55 | 8.20 |
| 8 | 13.55 | 1.16 | 0.59 | 9.34 |
| 9 | 13.45 | 1.14 | 0.58 | 8.82 |
| 10 | 12.60 | 1.13 | 0.52 | 7.36 |
| Average | 12.8 ± 0.4 | 1.17 ± 0.04 | 0.55 ± 0.02 | 8.3 ± 0.6 |

[S1] (a) W. Tress, *Adv. Energy Mater.* **2017,** *7*, 1602358; (b) M. Stolterfoht, C. M. Wolff, J. A. Márquez, S. Zhang, C. J. Hages, D. Rothhardt, S. Albrecht, P. L. Burn, P. Meredith, T. Unold, D. Neher, *Nat. Energy* **2018,** *3*, 847.